Accepted Manuscript

Chorionic and amniotic membrane-derived stem cells have distinct, and gestational diabetes mellitus independent, proliferative, differentiation, and immunomodulatory capacities

Liyun Chen, Marwan M. Merkhan, Nicholas R. Forsyth, Pensee Wu

PII:	S1873-5061(19)30167-9
DOI:	https://doi.org/10.1016/j.scr.2019.101537
Article Number:	101537
Reference:	SCR 101537
To appear in:	*Stem Cell Research*
Received date:	8 January 2019
Revised date:	25 June 2019
Accepted date:	12 August 2019

Please cite this article as: L. Chen, M.M. Merkhan, N.R. Forsyth, et al., Chorionic and amniotic membrane-derived stem cells have distinct, and gestational diabetes mellitus independent, proliferative, differentiation, and immunomodulatory capacities, Stem Cell Research, https://doi.org/10.1016/j.scr.2019.101537

Chorionic and amniotic membrane-derived stem cells have distinct, and gestational diabetes mellitus independent, proliferative, differentiation, and immunomodulatory capacities

Liyun Chen[1] l.chen1@keele.ac.uk, Marwan M. Merkhan[1,4] marwanmerkhan@gmail.com, Nicholas R. Forsyth[1,*] n.r.forsyth@keele.ac.uk, and Pensee Wu[1,2,3] p.wu@keele.ac.uk

[1]Guy Hilton Research Centre, Institute for Science and Technology in Medicine, Keele University, Stoke-on-Trent, U.K

[2]Academic Unit of Obstetrics and Gynaecology, University Hospital of North Midlands, Stoke-on-Trent, U.K

[3]Keele Cardiovascular Research Group, Institute for Applied Clinical Sciences and Centre for Prognosis Research, Institute of Primary Care and Health Sciences, Keele University, Stoke-on-Trent, U.K

[4]College of Pharmacy, University of Mosul, Mosul, Iraq

[*]Corresponding author.

Abstract

Placental membrane-derived mesenchymal stem cells (MSCs), with the advantages of being non-invasive and having fewer ethical issues, are a promising source for cell therapy. Gestational diabetes (GDM) alters the uterine environment and may affect the therapeutic potential of MSCs derived from placenta. Therefore, we evaluated the biological properties of amniotic (AMSCs) and chorionic membrane MSCs (CMSCs) from human GDM placenta in order to explore their therapeutic potential. In comparison of GDM-/Healthy- CMSCs and AMSCs, the immunophenotypes and typical stellate morphology of MSC were similar in CMSCs irrespective of disease state while the MSC morphology in GDM-AMSCs was less evident. GDM- and Healthy- CMSCs displayed an enhanced proliferation rate and tri-lineage differentiation capacity compared with AMSCs. Notably, GDM-CMSCs had a significantly increased adipogenic ability than Healthy-CMSCs accompanied by increased transcriptional responsiveness of *PPARγ* and *ADIPOQ* induction. The secretome effect of Healthy- and GDM- CMSCs/AMSCs by using conditioned media and coculture experiments, suggests that GDM- and Healthy- CMSCs provided an equivalent immunoregulatory effect on suppressing T-cells activation but a reduced effect of GDM-CMSCs on macrophage regulation. However, Healthy- and GDM- CMSCs displayed a superior immunomodulatory capacity in regulation of both T-cells and macrophages than AMSCs. In summary, we highlight the importance of the maternal GDM intrauterine environment during pregnancy and its impact on CMSCs/AMSCs proliferation ability, CMSCs adipogenic potential, and macrophage regulatory capacity.

Keywords: Gestational diabetes mellitus (GDM), placental membrane, amniotic MSC, chorionic MSC, adipogenesis, immunomodulation

Abbreviations

ADIPOQ, adiponectin; AMSCs, amniotic mesenchymal stem cells; CCL-17, chemokine (C-C motif) ligand 17; CMSCs, chorionic mesenchymal stem cells; CXCL-8, chemokine (C-X-C motif) ligand 8; GAPDH, glyceraldehyde-3-phosphate dehydrogenase; GDM, gestational diabetes mellitus; MRC1, mannose receptor C-type 1; MSC, mesenchymal stem cell; OD, optical density; PHA, phytohaemagglutinin; PMA, phorbol 12-myristate 13-acetate; PPARG, peroxisome proliferator activated receptor gamma

Introduction

Safe, effective, and reliable cell sources remain a major issue for use in regenerative medicine clinical applications. Bone marrow mesenchymal stem cells (MSCs) have now been widely and successfully used in clinical applications for a number of decades (Deans and Moseley, 2000). However, the limitations of adult stem cells have caused concerns, including their limited expansion capacities, scarcity within bone marrow, and the invasive and labour intensive isolation process which can associate with an increased risk of infection for the donor (Pittenger et al., 1999). Thus far, MSC derivation has been reported from a wider range of adult tissues including; fat, dental, and lung tissues and peripheral blood (Mimeault and Batra, 2006). The human placenta is also a plentiful and alternative source of stem cells (Pipino et al., 2013).

The human placenta plays a vital role in fetal development and maternal health by regulating the metabolic interaction between the mother and fetus. As the intrauterine environment is closely related to placental state, pregnant complications have been associated with abnormal placentation (Hsiao and Patterson, 2012; Kim et al., 2014b). Gestational diabetes mellitus (GDM) is a common complication of pregnancy affecting up to 13% of all

pregnancies worldwide (Zhu and Zhang, 2016). It is defined as glucose intolerance resulting in hyperglycaemia with onset during pregnancy, and shares similar features to type 2 diabetes (Buchanan et al., 2007). Its prevalence is increasing due to changing pregnancy population demographics, such as maternal age, body mass index and changing dietary habits (Ferrara, 2007; Hunt and Schuller, 2007). GDM affects both the mother and fetus during pregnancy, where maternal hyperglycaemia increases fetal weight and the risk of macrosomia (Kc et al., 2015). Although GDM resolves following delivery, women who had a history of GDM remain at an increased risk of developing type 2 diabetes in later life. Similarly, offspring from GDM pregnancies have a higher risk of developing type 2 diabetes in adulthood (Bellamy et al., 2009; Boney et al., 2005).

Given the environmental differences between GDM and healthy pregnancies, it is likely that MSCs derived from placentas will be affected by pregnancy complications. For example, a recent study reported the increased proportion of haematopoietic stem cells in cord blood of GDM pregnancy new-borns (Hadarits et al., 2016). In addition, perivascular stem cells from GDM pregnancy umbilical cords had lower cell yields and proliferative rate when compared to healthy pregnancies (An et al., 2017). Environmental factors can cause significant effects on cell populations and behaviours; therefore, understanding the biological properties of stem cells is important before applying these cells in clinical applications.

Placental stem cells with the ease of access, reduced ethical conflicts, and reduced age-acquired DNA damage (Tsagias et al., 2011), are phenotypically similar to bone marrow derived MSCs, including plastic adhesion, immunophenotype, and lineage differentiation potential. In addition, it has also been suggested that the placental MSC provides a substantial expansion potential and delayed senescence (Brooke et al., 2008; Hass et al., 2011). The

placental membranes are formed from the extraembryonic mesoderm, and consist of the chorionic and the amniotic membranes. The chorionic (maternal side) and amniotic (fetal side) membrane are loosely connected together to line the amniotic cavity enclosing the fetus, from where chorionic mesenchymal stem cells (CMSCs) and amniotic mesenchymal stem cells (AMSCs) are isolated, respectively (Parolini et al., 2008). The amniotic membrane itself is used widely as a biomaterial for the treatment of burns, skin, and corneal transplantation, due to its anti-inflammatory, anti-microbial, anti-scarring, and anti-angiogenic properties (Mamede et al., 2012). The AMSCs present in the amniotic membrane help in regenerating damaged tissues via regulation of the immune response to facilitate transplantation and associated reductions in inflammation (Kim et al., 2014a). The chorionic membrane, also a rich source of MSC, remains poorly understood.

Considering the importance of environmental impacts on MSC development, understanding fundamental biological properties is an essential first step to evaluate the therapeutic potential of each type of MSCs. In this study, explored the differences in the biological characteristics between CMSCs and AMSCs as well as the comparisons between GDM and Healthy pregnancies in order to provide further mechanistic understanding of GDM-/Healthy- CMSCs and AMSCs.

Materials and methods

Human tissue samples

All placentas in our research were collected from Royal Stoke University Hospital, UK, after obtaining Research Ethics Committee and Health Research Authority approvals (Reference 15/WM/0342). Women undergoing Caesarean sections provided written informed consent to donate their placenta. Term placenta were collected from healthy donors (n=9) and

donors with GDM (*n*=9). The CMSCs/AMSCs isolation process was performed within an hour of collecting the placenta from Caesarean section, using the protocol by Marongiu et al (Marongiu et al., 2010).

Isolation and culture of CMSCs/AMSCs and immune cells

Amniotic membrane was manually peeled from the underlying chorionic membrane. As chorionic membrane is attached to maternal tissues, a removal of decidual tissue was required. The membranes were washed with PBS to remove blood clots and then placed in 0.05% trypsin/EDTA solution at 37°C for 1 h. Membranes were then washed with PBS and followed by digestion with Collagenase type IV (Thermo Scientific, USA) at 37°C for 1-1.5 h. During the digestion process, the membranes were checked every 15 mins and the incubation was stopped once the membranes were completely dissolved. The mobilised cells were collected by centrifugation at 200g for 5 min, resuspended in Dulbecco's Modified Eagle's Medium (DMEM; Lonza, UK) consisting of 1% L-glutamine, 10% fetal bovine serum, 1% Penicillin-Streptomycin, and 1% non-essential amino acids (NEAA) and seeded at the density of 1×10^5 cells per cm^2. The immune cells lines, Jurkat and THP1 were obtained from Institute of Science and Technology in Medicine (Keele University, UK) and cultured in RPMI 1640 medium (Lonza, UK) supplemented with 10% fetal bovine serum and 1% Penicillin-Streptomycin.

Characterisation of CMSCs and AMSCs

CMSCs and AMSCs derived from GDM and healthy placenta were characterised through morphology analysis, cell surface marker expression by immunophenotypic analysis, and *in vitro* osteogenic, adipogenic and chondrogenic differentiation.

Cell morphology analysis

Changes in cell morphology were detected by Olympus microscope and images were processed with Image-Pro Insight software. To analyse the cell length and surface area, 5 images were taken from each sample from passage 0-2. Single cells that appeared clearly separated were used for analysis by Image J. Cell length was measured of the longest axis from the cell periphery.

Immunophenotyping analysis

Cells were harvested at passage 3 for analysis. Ten phycoerythrin (PE) conjugated antibodies (CD73, CD90, CD105, CD14, CD19, CD34, CD45, and HLA, IgG1 and IgG2 (Miltenyi Biotec, Germany) were used– following the manufacturer's recommended antibody volumes. MSCs were characterised using flow cytometry (Beckman Coulter Cytomics FC 500 and CXP software, USA) and flow cytometry data were processed with Flowing Software 2.

Trilineage differentiation

Cells at the second passage were seeded and cultured in standard culture condition. Following cell adherence, the medium was replaced with a differentiation medium, which was changed every 3 days during the 21-day culture.

To induce osteogenic differentiation and adipogenic differentiation, 2×10^4 cells/well were seeded in 24-well plate and cultured in differentiation medium. Both differentiation medium used contained DMEM with 10% FBS, 1% L-glutamine, and 1% NEAA. For osteogenesis, medium was supplemented with 50 μM ascorbic acid, 10 mM β-glycerol phosphate, and 0.1 μM dexamethasone. For adipogenesis, medium was supplemented with 0.5 μM dexamethasone, 0.5 mM isobutylxanthine, 10 μg/ml insulin, and 100 μM indomethacin. To induce chondrogenic differentiation, 1 x 10^5 hMSC were resuspended in 8 μl of medium and dropped in the centre of the well as a micromass. After 1-hour incubation in the standard culture condition to allow cells to adhere with the culture surface,

micromasses were then replenished with chondrogenic differentiation media, consisting of DMEM with 1% FBS, 1% L-glutamine, 1% NEAA and supplemented with 1% ITS, 0.1 μM dexamethasone, 50 μM ascorbic acid, 40 μg/mL L-proline, 1% sodium pyruvate, and 10 ng/mL transforming growth factor 3 (TGF-3; Peprotech, UK). To evaluate the trilineage differentiation, the mineral deposition of differentiated osteoblasts was detected by Alizarin red; lipid accumulation in adipocytes was stained with Oil-Red-O; and proteoglycan-rich matrix accumulation in chondrocytes was detected by Alcian Blue. All the chemicals used were obtained from Sigma-Aldrich, USA.

RNA extraction and real-time PCR

Total RNA was isolated by Trizol Reagent (Invitrogen, USA), according to the manufacturer's instruction. Complementary DNA was prepared from 1 μg of total RNA using High-Capacity cDNA Reverse Transcription Kit (Thermo Scientific, USA). Gene expression analysis was evaluated by real-time PCR using QuantiFast SYBR Green PCR Kit (Qiagen, Germany). Primer sequences for each gene are shown in Table 2. The relative expression levels of mRNA were normalized to *GAPDH* and the fold difference was calculated using the $\Delta\Delta C_t$ method compared with controls.

Cell growth and proliferation

Cell numbers were counted every 2 days and the doubling time was calculated. Equation for doubling time = (T2-T1) × log 2/ (log N2 – log N1), where: T1, final time (hours); T2, initial time; N1, initial cell numbers; and N2, final cell numbers. Cell proliferation was conducted by 3-(4,5-dimethylthiazol-2-yl)-2,5-diphenyltetrazolium bromide (MTT) assay (Sigma, USA), according to the manufacturer's instruction. The absorbance of the samples was read at wavelengths of 570 nm. The results are presented as the mean ± SD

of triplicates, taking time as the horizontal axis and Optical density (OD) as the longitudinal axis. Cell viability was examined by using 0.4% trypan blue (Sigma) exclusion for living cells. The percentage of cell death was calculated by counting blue-coloured cells (dead cell) from a total number of 100 cells in a haemocytometer.

PMA-THP1/MSC co-culture

The effects of CMSCs/AMSCs on macrophage to M1 or M2 differentiation were evaluated by a co-culturing system. THP-1 cells were pre-treated with 50 ng/ml phorbol 12-myristate 13-acetate (PMA; Sigma) for 24 h, washed with PBS to remove PMA and cultured in 50% RPMI and 50% DMEM, containing 10% FBS for 24 h to induce differentiation to macrophage. To co-culture PMA-THP1 with CMSCs or AMSCs, both cells were physically separated by cell-culture inserts (0.4 μM pore size, Millipore, Germany). PMA-THP1 were seeded at a density of 5×10^5 cells/well to 12-well plates and treated with 20 ng/ml INFγ and 10 pg/ml lipopolysaccharide (LPS) to induce M1 macrophage, 20 ng/ml IL-4 for M2 macrophage or co-cultured with 5×10^5 CMSCs/AMSCs. PMA-THP1 cells were placed in the lower layer and CMSCs/AMSCs were added to the upper layer. After co-culturing for 24 h, RNA was extracted for real-rime PCR and the supernatants were collected for Elisa assay.

Cytokines release and Enzyme Linked Immunosorbent Assay (ELISA)

Jurkat T cells were stimulated with 5 μg/ml phytohaemagglutinin (PHA; Sigma) plus 50 ng/ml phorbol 12-myristate 13-acetate (PMA; Sigma) to induce IL-2 release. THP1 cells were pre-treated with 50 ng/ml PMA and then treated with INFγ or IL-4 to induce TNF-α and IL-10 secretion, respectively. Supernatants were collected and tested for the presence of IL-2, IL-10, and TNF-α by Human TMB ELISA Development kit (Peprotech, UK) following the manufacturer's instruction.

Statistical analysis

One-way ANOVA and Tukey post-hoc tests or two-way ANOVA were used to determine the statistical significance of observed differences in the mean values among different groups by GraphPad Prism (GraphPad Software). The data was presented as mean ± SEM. Each data point represents the average of at least three independent experiments with three repeats in each experiment. A *p*-value below 0.05 was indicated as statistically significant (*$p \leq 0.05$, **$p \leq 0.01$, ***$p \leq 0.001$ and ****$p \leq 0.0001$).

Results

AMSCs and CMSCs have distinct morphologies independent of disease state

AMSCs and CMSCs lines derived from healthy (n=9) and GDM (n=9) placenta were used in this study. The details of each pregnancy are shown in Table 1.

We compared MSC morphology in healthy and GDM pregnancies. CMSCs form healthy (H-MSCs) and GDM (G-CMSCs) pregnancies exhibited similar fibroblast-like morphologies from passage 0 and maintained the stable morphological features during the subsequent culture (Fig. 1A). Conversely, the morphology of AMSCs differed between healthy (H-AMSCs) and GDM (G-AMSCs) groups where the H-AMSCs displayed a triangular or spindle shapes after seeding for 24 hours and the G-AMSCs, which attached more slowly, displayed reduced adherence and a more cuboidal shape (Fig. 1B). The CMSC length (the longest axis from the cell periphery) gradually increased and was longer than AMSCs between passage 0 to 2. The morphology of AMSCs became elongated in the subsequent passages, where more fibroblast-shaped cells were detected. Comparison between GDM and healthy pregnancies demonstrated that G-CMSC displayed comparable length to H-CMSCs (Fig. 1C), while G-AMSCs were shorter than H-AMSCs (Fig. 1D). Surface area

measurement indicated that AMSCs displayed a larger and broader surface area, on average s than CMSCs. There was no significant difference in surface areas between CMSCs or AMSCs taken from healthy and GDM pregnancies (Fig. 1E). We investigated whether the morphological differences were associated with MSCs phenotypic changes over the culture period via the examination of pluripotent (*NANOG, OCT4*), endodermal (*SOX7, SOX17*), mesodermal (*FOXC1, TBX6*), and ectodermal (*NES, OTX2*) lineage markers in H-/G- CMSCs/AMSCs from passage 0-3. Pluripotent and endodermal markers were detectable in H-/G- CMSCs/AMSCs at early passages while the expression significantly reduced at late passages. Likewise, H-/G- CMSCs/AMSCs also expressed mesodermal lineage markers at early passage but the expression levels remained high at passage 3. Notably, *FOXC1* and *TBX6* were significantly higher in H-/G- CMSCs vs. H-/G- AMSCs at passage 1-2 and 2-3, respectively. Ectodermal lineage markers were undetectable in both H-/G- CMSCs and AMSCs. Collectively, with the reduction of pluripotent and endodermal markers but not mesodermal markers, H-/G- CMSCs and ASMCs appear to become increasingly committed to a mesodermal phenotype with increasing passage number (Fig. 2 and Fig. S1).

CMSCs display an increased proliferative rate than AMSCs while GDM has an opposite impact on CMSCs and AMSCs doubling rates

The proliferation capacity was evaluated during a 12-day culture window. H-CMSCs and G-CMSCs both evidenced a short lag-phase at day 0-4, followed by an exponential growth curve from days 4-12. On the other hand, the cell numbers of H-AMSCs and G-AMSCs slowly increased for the first 8 days and gradually reached plateau from day 8-12 (Fig. 3A). A lower proliferation capacity was exhibited in H-/G- AMSCs with a doubling time of 91.4 hours for H-AMSCs and 81.6 hours for G-AMSCs compared to CMSCs from healthy and GDM placenta with doubling times of 37.9 hours and 44.0 hours, respectively (Fig. 3B). The

data indicated that CMSCs proliferate more rapidly than AMSCs and comparing the healthy and GDM group, G-CMSCs showed lower growth ability than H-CMSCs while AMSCs displayed the converse.

A reduced metabolic activity in G-CMSCs was observed when compared to H-CMSC through the detection of cleaved MTT by metabolically active cells (Fig. 3C). This may simply reflect the reduced cell counts observed in the G-CMSCs population. However, between H-AMSCs and G-AMSCs the converse was noted where G-AMSCs showed a relatively higher metabolic level than H-AMSCs which was consistent with both previous cell number and doubling time observations (Fig. 3B-C). Cell viability was determined by trypan blue staining for non-viable cells during the time period measured with MTT. This showed 8-10% cell death in H-/G- CMSCs and AMSCs with no significant difference between time points in each group (Fig. S2). Overall, an enhanced proliferation ability was seen in H-/G-CMSCs than H-/G-AMSCs, where H-CMSCs showed an increased proliferation rate than G-CMSCs whereas the opposite was observed between H-AMSCs and G-AMSCs.

GDM CMSCs/AMSCs and healthy CMSCs/AMSCs immunophenotypes are broadly comparable

The immunophenotype of H-/G- CMSCs and AMSCs were comparable and displayed high levels of expression of typical MSC markers; CD73, CD90, CD105, and low levels of CD14, CD19, CD34, CD45 and HLA-DR. There was no significant difference between CMSCs and AMSCs in either GDM or healthy groups. However, CD45 expression was significantly higher in G-CMSCs/AMSCs when compared to their healthy counterparts; 17.5% ± 2.0% in G-CMSCs, 7% ± 2.6% in H-CMSCs and 16% ± 1.0% in G-AMSCs, 6.3% ± 1.5% in H-AMSCs (Fig. 3D and Fig. S3).

GDM environment promotes MSC lineage commitment toward adipogenesis

H-/G- CMSCs and AMSCs were exposed to specific differentiation media to induce tri-lineage differentiation as identified by histological staining (Fig. 4A). CMSCs from healthy and GDM placentas both exhibited a differentiation capacity towards all lineages examined. Osteogenic and chondrogenic differentiation were comparable between both CMSCs and AMSCs from healthy and GDM placentas. In contrast H-AMSCs and G-AMSCs displayed little or no adipogenic differentiation potential (Fig. 4B and Fig. S4). Quantification of Oil-Red-O confirmed the histological observations with significantly more intense staining in G-CMSCs after differentiation for 21 days (Fig. 4C).

To investigate enhanced adipogenic differentiation potential in MSCs from GDM placenta, the basal levels of two adipogenic-associated factors, *PPARγ* and *ADIPOQ*, were examined before the induction for adipogenesis. G-CMSCs and G-AMSCs both showed a 2 to 3-fold increase in *ADIPOQ* basal expression levels vs. healthy CMSCs/AMSCs (Fig. 4D). Likewise, higher *PPARγ* expression was exhibited in G-CMSCs than H-CMSCs (Fig. 4E). We further investigated the expression of *PPARγ* and *ADIPOQ* during adipogenesis at six different time points (day 0, 7, 10, 14, 17, 21). *PPARγ* and *ADIPOQ* expression in H-/G-CMSCs displayed elevation across the differentiation time course, peaking at day 14 and *PPARγ* decreasing thereafter while *ADIPOQ* remaining elevated (Fig. 4F-G). During adipogenic differentiation G-CMSCs expressed significantly higher levels of both *PPARγ* and *ADIPOQ* than H-CMSCs at every time point. Notably *ADIPOQ* was initially higher in G-AMSCs than H-AMSCs but no significant induction during the differentiation period was seen (Fig. 4F). *PPARγ* displayed some upregulation in H-/G- AMSCs but not to levels seen with CMSCs (Fig. 4G). This indicates that H-/G-AMSCs have a limited adipogenic capacity in spite of G-AMSCs displaying increased basal expression levels of *ADIPOQ* and *PPARγ*.

Conditioned media from H-/G- CMSCs and AMSCs has a significant antiproliferative effect on T-cells

To evaluate the immunoregulatory properties of healthy and GDM CMSCs/AMSCs the proliferation and inflammatory cytokines secretion of T-cells were investigated. Jurkat cells cultured in complete growth media (10%FBS) showed a steady increase in proliferation; however, a significant reduction in numbers was noted following on from exposure to either H-/G- CMSC or AMSCs conditioned media (CM) (Fig. 5A). PHA/PMA activated Jurkat cells also displayed a sensitivity to H-/G- CMSCs and AMSCs CM and similarly displayed a reduced proliferation rate following on from exposure (Fig. 5B). Noteworthy was that though CM from both H-/G- CMSCs and AMSCs suppressed Jurkat proliferation this was to a significantly greater extent with CM from H-/G- CMSCs. No differences were noted between healthy and GDM groups. Interleukin-2, produced from PHA/PMA stimulation, regulates proliferation and differentiation of activated T-cells. The supernatant from activated Jurkat cells cultured in H-/G- CMSCs CM contained significantly reduced levels of secreted IL-2. H-/G-AMSCs CM also suppressed IL-2 secretion; however, the suppressive effect was lower than that of H-/G-CMSCs CM (Fig. 5C).

Distinct immunoregulatory properties of Chorionic MSCs evaluated by macrophage modulation

MSCs modulate immune cell function through a variety of mechanisms. Macrophages are key regulators of initiation and control of inflammation, and are typically divided into two types: classically activated type 1 macrophages (M1), characterised by the production of pro-inflammatory cytokines with an acute inflammatory phenotype, and alternatively activated type 2 macrophages (M2), secreting anti-inflammatory cytokines (Mantovani et al., 2004).

THP-1 monocytes were differentiated into macrophages using PMA (PMA-THP1, M0) followed by co-culture with H-/G- CMSCs or AMSCs. PMA-THP1 was activated by interferon-γ (IFN-γ) and lipopolysaccharide (LPS) in order to obtain M1 polarized macrophages or interleukin 4 (IL-4) for M2 polarization (Fig. 6A). Following co-culture of H-/G- CMSCs or AMSCs with PMA-THP1, THP1 were collected to examine the macrophage polarization. Inflammatory M1 macrophages express high levels of inflammatory markers, including *IL-1β, IL-12*, *CXCL8,* and *TNF* (Fig 6B-E). When co-cultured with H-/G- CMSCs or AMSCs, there was no significant increase in *IL-1β or IL-12* inflammatory marker expression though some slight, significant, increases were noted for each these were either equivalent to or below control (Fig. 6B-C). Notably, *CXCL8* and *TNF* were induced in PMA-treated THP1 while the expression was significantly suppressed after co-culturing with H-/G- CMSCs/AMSCs (Fig. 6D-E).

On the other hand, anti-inflammatory M2 macrophages are characterised by increased expression of *IL-10, MRC1*, and *CCL-17*. High levels of M2 macrophage markers were detected when PMA-THP1 were co-cultured with CMSCs or AMSCs (Fig. 6F-H). Co-culture with H-/G- CMSCs produced significantly higher expression of *MRC1* and *CCL-17* than co-culture with H-/G- AMSCs suggesting that CMSCs had a more profound effect on promoting M2 polarization than AMSCs. Moreover, no significant difference was detected in the ability to induce M2 macrophage differentiation in H-/G- AMSCs but in CMSCs higher *MRC1* and *CCL-17* expression could be observed in H-CMSCs than with G-CMSCs (Fig 6G-H)

We further examined the pro-inflammatory cytokines, TNF-α, and anti-inflammatory cytokine, IL-10, which are secreted by M1 and M2 macrophage, respectively. No significant increase in TNF-α secretion (Fig. 7A) was seen but an upregulation in IL-10 (Fig. 7B) was detected when co-culturing PMA-THP1 with H-/G- CMSCs or AMSCs. Corresponding with M2 markers gene expression, we found that CMSCs and AMSCs derived from healthy or

GDM placenta were capable of promoting PMA-THP1 towards M2 polarization. Overall, H-/G- CMSC displayed superior immunosuppressive capacity in modulating T cells and macrophages than H-/G- AMSCs. The GDM environment did not alter macrophage regulation ability in AMSCs though slightly attenuated the immunoregulatory effect of G-CMSCs.

Discussion

The placenta that is usually discarded after delivery, is a valuable source of plentiful perinatal MSCs for regenerative medicine with few ethical issues. Cell therapy with placental-derived MSCs have already been applied to treat various disorders in animal models (Oliveira and Barreto-Filho, 2015) and some clinical applications, such as ischaemic stroke, Crohn's disease, and idiopathic pulmonary fibrosis (Antoniadou and David, 2016; Pipino et al., 2013; Trounson and McDonald, 2015). However, few studies have investigated the differences in therapeutic potential between CMSCs and AMSCs. Chorionic and amniotic MSCs are developed from extraembryonic tissue and can be isolated from different layers of the placental membrane. The placental membrane contains both fetal and maternal components which may be a potential source of autologous treatment for both mother and child. In this study, we provided a thorough comparison of CMSCs and AMSCs; and to our knowledge, are the first to report the varying effects of the GDM environment in CMSCs and AMSCs.

Derived from different layers of the same placental membrane, CMSCs and AMSCs display diverse biological characteristics. The elongated morphology of H-/G-CMSCs may be associated with enhanced differentiation potential towards certain lineages. During development, embryonic mesenchymal cell elongation initiates visceral myogenesis (Yang et al., 1999). Elongated morphology of bone-marrow MSCs showed enhanced ability towards

smooth muscle cells differentiation and tenogenic differentiation (Hamilton et al., 2004; Wang et al., 2013). Moreover, cell mobilisation is also characterised by an elongated cell morphology as the initial step for cell migration (Brabek et al., 2010; Friedl and Wolf, 2010). Increased cell length may indicate some enhanced MSC properties in H-/G-CMSCs vs H-/G-AMSCs.

The reduced proliferation rate of AMSCs compared with CMSCs is consistent with previous reports indicating the limited *ex vivo* expansion potential of AMSCs (Jaramillo-Ferrada et al., 2012). We further investigated the difference in growth ability between GDM and healthy CMSCs/AMSCs. It has been suggested previously that umbilical cord derived-MSCs from GDM women displayed decreased cell growth with early cellular senescence accompanied by expression of p16 and p53 (Kim et al., 2015). Alternatively, Pierdomenico et al. described MSCs obtained from umbilical cord of both healthy and diabetic mothers where the later demonstrated an increased proliferative ability along with an upregulation of CD44, CD29, CD73, CD166, SSEA4 and TERT (Pierdomenico et al., 2011). We explored the GDM effect on CMSCs and AMSCs proliferation which indicated that G-CMSCs displayed reduced rates when compared to H-CMSCs while G-AMSCs, by contrast, showed higher proliferation rates than H-AMSCs. As AMSCs are derived from the amniotic membrane adjacent to the fetus, the higher proliferation rate of diabetic AMSCs may reflect features of GDM including heavier fetal weights on resultant cell phenotype.

Emerging research has highlighted the importance of the intrauterine environment as a risk factor in the likelihood of offspring developing obesity and metabolic diseases (Gaillard, 2015; Tamashiro and Moran, 2010). The underlying biological mechanism for the link between GDM and the increased risk of future diabetes is poorly understood, although the GDM environment has potential to modify the epigenetic state of fetal genes. Increased

methylation of *PYGO1* and *CLN8* genes in offspring exposed to a GDM environment is proposed as being associated with long-term adverse effects on fetal health (Lehnen et al., 2013; West et al., 2013). GDM is associated with newborn hyperinsulinemia with effects on offspring fat mass seen until 6 weeks. Elevated preperitoneal adipose tissue in newborns is linked with increased risk of obesity in later life (Uebel et al., 2014). We found that the CMSCs and AMSCs differentiation potential are influenced by maternal environment during gestation. Under the same culture condition, elevated adipogenic differentiation was found in GDM-MSCs than with MSCs from healthy pregnancies. Moreover, higher basal expression levels of adipogenic-associated genes in G-CMSCs and subsequent lipid content associated with increased transcription factor expression during differentiation indicated an enhanced adipogenic potential when compared to H-/G- AMSCs. This suggests that the GDM environment itself may have less of a role in affecting fetal cell properties than that of the membrane itself.

For successful clinical application of MSC therapy, the immunoregulatory potential of CMSCs and AMSCs is an important area of consideration. The immune responses mediated by T-cells may lead to cell transplant rejection or Graft-Versus-Host disease (Ingulli, 2010). MSCs have been reported to modulate the proliferation and function of immune cells by both cell-to-cell contact and the secretion of growth factors, cytokines, and chemokines (Kyurkchiev et al., 2014). Given that the placenta plays a critical role in fetomaternal tolerance and contains cells that display immunomodulatory properties, MSCs derived from placenta not only have superior immunomodulatory potential but also have therapeutic potential for the mothers and offspring (Ilancheran et al., 2009; Talwadekar et al., 2015). In our finding, CMSCs and AMSCs displayed differential levels of immunosuppressive capacities. H-/G- CMSCs showed superior immunosuppressive ability in inhibiting Jurkat cells proliferation and IL-2 secretion than with AMSCs. Moreover, MSCs are also involved in

regulating the innate immune response by modulating macrophage polarization and inhibition of inflammatory cytokines secretions (Glenn and Whartenby, 2014; Spaggiari and Moretta, 2013). H-/G- CMSCs promoted macrophage differentiation toward M2 polarization and induced higher M2 marker expression than H-/G- AMSCs. Both CMSCs and AMSCs from healthy or GDM placenta possessed immunoregulatory properties, however, better immunosuppressive potential was observed in CMSCs than with AMSCs, particularly in CMSCs from healthy placenta. Several studies have already demonstrated the immunosuppressive potential of AMSCs, where they were able to inhibit LPS-induced inflammatory cytokines secretion by macrophages through the suppression of NF-Kb (Shu et al., 2015). However, we are the first to compare the immunosuppressive effect between H-/G-CMSCs and AMSCs. Notably, the GDM environment had no significant effect on the immunosuppressive ability of MSCs. Despite an increase in M2 marker expressions after co-culturing THP1 with H-CMSCs, which might suggest a better macrophage modulation potential in H-CMSCs than G-CMSCs, G-CMSCs showed a competitive ability in regulating Jurkat activity and modulating cytokine secretion. Likewise, the responses from Jurkat cells treated with G-AMSCs conditioned media or macrophages co-cultured with G-AMSCs were similar to the result from H-AMSCs.

In summary, human placenta is comprised of several stem cells niches that mostly originate from extraembryonic tissue, and connect to maternal tissues, which may be a promising autologous source for cell therapy in both the mother and her offspring. Bone marrow MSCs isolated from elder donors have been reported to have reduced biological activity, thus leading to poor therapeutic potential (Mueller and Glowacki, 2001). Insufficient numbers of MSCs or impaired MSCs function from patients with rheumatoid arthritis and diabetes, respectively, have also been reported (Cianfarani et al., 2013; Sun et al., 2015). Therefore, an understanding of MSC behaviour under different growth environment is

essential. In this study, we provide a comparison between CMSCs and AMSCs from healthy and GDM placenta, and evaluate the biological characteristics of both. This information could contribute to the future development of autologous cell therapy for women or children from GDM pregnancies and regenerative medicine approaches of using MSCs derived from GDM placenta.

Conclusions

CMSCs and AMSCs have distinct biological properties. The superior proliferation, differentiation and immunomodulatory properties in CMSCs than AMSCs make them a promising alternative source for autologous cell transplantation. In addition, we demonstrated the importance of the maternal GDM intrauterine environment and its differential effects on CMSCs and AMSCs.

Authors' contributions

All authors contributed to experimental design. LC acquired, analysed and interpreted the data and wrote the manuscript. MMM contributed to data acquisition and analysis. NRF and PW supervised the study, interpreted the data, and revised the manuscript. PW coordinated the sample collections from individuals. All authors approved the final version of the manuscript and are responsible for the integrity of the work as a whole.

Competing interests

The authors declare that they have no competing interests.

Funding

This work was funded by an ISTM/ACORN research grant from Keele University and Iraqi Ministry of Higher Education and Scientific Research.

References

An, B., Kim, E., Song, H., Ha, K.S., Han, E.T., Park, W.S., Ahn, T.G., Yang, S.R., Na, S., and Hong, S.H. (2017). Gestational Diabetes Affects the Growth and Functions of Perivascular Stem Cells. Mol Cells *40*, 434-439.

Antoniadou, E., and David, A.L. (2016). Placental stem cells. Best Pract Res Clin Obstet Gynaecol *31*, 13-29.

Bellamy, L., Casas, J.P., Hingorani, A.D., and Williams, D. (2009). Type 2 diabetes mellitus after gestational diabetes: a systematic review and meta-analysis. Lancet *373*, 1773-1779.

Boney, C.M., Verma, A., Tucker, R., and Vohr, B.R. (2005). Metabolic syndrome in childhood: association with birth weight, maternal obesity, and gestational diabetes mellitus. Pediatrics *115*, e290-296.

Brabek, J., Mierke, C.T., Rosel, D., Vesely, P., and Fabry, B. (2010). The role of the tissue microenvironment in the regulation of cancer cell motility and invasion. Cell Commun Signal *8*, 22.

Brooke, G., Tong, H., Levesque, J.P., and Atkinson, K. (2008). Molecular trafficking mechanisms of multipotent mesenchymal stem cells derived from human bone marrow and placenta. Stem Cells Dev *17*, 929-940.

Buchanan, T.A., Xiang, A., Kjos, S.L., and Watanabe, R. (2007). What is gestational diabetes? Diabetes Care *30 Suppl 2*, S105-111.

Cianfarani, F., Toietta, G., Di Rocco, G., Cesareo, E., Zambruno, G., and Odorisio, T. (2013). Diabetes impairs adipose tissue-derived stem cell function and efficiency in promoting wound healing. Wound Repair Regen *21*, 545-553.

Deans, R.J., and Moseley, A.B. (2000). Mesenchymal stem cells: biology and potential clinical uses. Exp Hematol *28*, 875-884.

Ferrara, A. (2007). Increasing prevalence of gestational diabetes mellitus: a public health perspective. Diabetes Care *30 Suppl 2*, S141-146.

Friedl, P., and Wolf, K. (2010). Plasticity of cell migration: a multiscale tuning model. J Cell Biol *188*, 11-19.

Gaillard, R. (2015). Maternal obesity during pregnancy and cardiovascular development and disease in the offspring. Eur J Epidemiol *30*, 1141-1152.

Glenn, J.D., and Whartenby, K.A. (2014). Mesenchymal stem cells: Emerging mechanisms of immunomodulation and therapy. World journal of stem cells *6*, 526-539.

Hadarits, O., Zoka, A., Barna, G., Al-Aissa, Z., Rosta, K., Rigo, J., Jr., Kautzky-Willer, A., Somogyi, A., and Firneisz, G. (2016). Increased Proportion of Hematopoietic Stem and Progenitor Cell Population in Cord Blood of Neonates Born to Mothers with Gestational Diabetes Mellitus. Stem Cells Dev *25*, 13-17.

Hamilton, D.W., Maul, T.M., and Vorp, D.A. (2004). Characterization of the response of bone marrow-derived progenitor cells to cyclic strain: implications for vascular tissue-engineering applications. Tissue Eng *10*, 361-369.

Hass, R., Kasper, C., Bohm, S., and Jacobs, R. (2011). Different populations and sources of

human mesenchymal stem cells (MSC): A comparison of adult and neonatal tissue-derived MSC. Cell Commun Signal *9*, 12.

Hsiao, E.Y., and Patterson, P.H. (2012). Placental regulation of maternal-fetal interactions and brain development. Dev Neurobiol *72*, 1317-1326.

Hunt, K.J., and Schuller, K.L. (2007). The increasing prevalence of diabetes in pregnancy. Obstet Gynecol Clin North Am *34*, 173-199, vii.

Ilancheran, S., Moodley, Y., and Manuelpillai, U. (2009). Human fetal membranes: a source of stem cells for tissue regeneration and repair? Placenta *30*, 2-10.

Ingulli, E. (2010). Mechanism of cellular rejection in transplantation. Pediatric nephrology *25*, 61-74.

Jaramillo-Ferrada, P.A., Wolvetang, E.J., and Cooper-White, J.J. (2012). Differential mesengenic potential and expression of stem cell-fate modulators in mesenchymal stromal cells from human-term placenta and bone marrow. J Cell Physiol *227*, 3234-3242.

Kc, K., Shakya, S., and Zhang, H. (2015). Gestational diabetes mellitus and macrosomia: a literature review. Ann Nutr Metab *66 Suppl 2*, 14-20.

Kim, E.Y., Lee, K.B., and Kim, M.K. (2014a). The potential of mesenchymal stem cells derived from amniotic membrane and amniotic fluid for neuronal regenerative therapy. BMB Rep *47*, 135-140.

Kim, H.S., Cho, S.H., Kwon, H.S., Sohn, I.S., and Hwang, H.S. (2014b). The significance of placental ratios in pregnancies complicated by small for gestational age, preeclampsia, and gestational diabetes mellitus. Obstet Gynecol Sci *57*, 358-366.

Kim, J., Piao, Y., Pak, Y.K., Chung, D., Han, Y.M., Hong, J.S., Jun, E.J., Shim, J.Y., Choi, J., and Kim, C.J. (2015). Umbilical cord mesenchymal stromal cells affected by gestational diabetes mellitus display premature aging and mitochondrial dysfunction. Stem Cells Dev *24*, 575-586.

Kyurkchiev, D., Bochev, I., Ivanova-Todorova, E., Mourdjeva, M., Oreshkova, T., Belemezova, K., and Kyurkchiev, S. (2014). Secretion of immunoregulatory cytokines by mesenchymal stem cells. World journal of stem cells *6*, 552-570.

Lehnen, H., Zechner, U., and Haaf, T. (2013). Epigenetics of gestational diabetes mellitus and offspring health: the time for action is in early stages of life. Mol Hum Reprod *19*, 415-422.

Mamede, A.C., Carvalho, M.J., Abrantes, A.M., Laranjo, M., Maia, C.J., and Botelho, M.F. (2012). Amniotic membrane: from structure and functions to clinical applications. Cell Tissue Res *349*, 447-458.

Mantovani, A., Sica, A., Sozzani, S., Allavena, P., Vecchi, A., and Locati, M. (2004). The chemokine system in diverse forms of macrophage activation and polarization. Trends Immunol *25*, 677-686.

Marongiu, F., Gramignoli, R., Sun, Q., Tahan, V., Miki, T., Dorko, K., Ellis, E., and Strom, S.C. (2010). Isolation of amniotic mesenchymal stem cells. Curr Protoc Stem Cell Biol *Chapter 1*, Unit 1E 5.

Mimeault, M., and Batra, S.K. (2006). Concise review: recent advances on the significance of stem cells in tissue regeneration and cancer therapies. Stem Cells *24*, 2319-2345.

Mueller, S.M., and Glowacki, J. (2001). Age-related decline in the osteogenic potential of human bone marrow cells cultured in three-dimensional collagen sponges. Journal of cellular biochemistry *82*, 583-590.

Oliveira, M.S., and Barreto-Filho, J.B. (2015). Placental-derived stem cells: Culture, differentiation and challenges. World J Stem Cells *7*, 769-775.

Parolini, O., Alviano, F., Bagnara, G.P., Bilic, G., Buhring, H.J., Evangelista, M., Hennerbichler, S., Liu, B., Magatti, M., Mao, N.*, et al.* (2008). Concise review: isolation and characterization of cells from human term placenta: outcome of the first international Workshop on Placenta Derived Stem Cells. Stem Cells *26*, 300-311.

Pierdomenico, L., Lanuti, P., Lachmann, R., Grifone, G., Cianci, E., Gialò, L., Pacella, S., Romano, M., Vitacolonna, E., and Miscia, S. (2011). Diabetes mellitus during pregnancy interferes with the biological characteristics of Wharton's jelly mesenchymal stem cells. The Open Tissue Engineering and Regenerative Medicine Journal *4*.

Pipino, C., Shangaris, P., Resca, E., Zia, S., Deprest, J., Sebire, N.J., David, A.L., Guillot, P.V., and De Coppi, P. (2013). Placenta as a reservoir of stem cells: an underutilized resource? Br Med Bull *105*, 43-68.

Pittenger, M.F., Mackay, A.M., Beck, S.C., Jaiswal, R.K., Douglas, R., Mosca, J.D., Moorman, M.A., Simonetti, D.W., Craig, S., and Marshak, D.R. (1999). Multilineage potential of adult human mesenchymal stem cells. Science *284*, 143-147.

Shu, J., He, X., Zhang, L., Li, H., Wang, P., and Huang, X. (2015). Human amnion mesenchymal cells inhibit lipopolysaccharide-induced TNF-alpha and IL-1beta production in THP-1 cells. Biological research *48*, 69.

Spaggiari, G.M., and Moretta, L. (2013). Cellular and molecular interactions of mesenchymal stem cells in innate immunity. Immunology and cell biology *91*, 27-31.

Sun, Y., Deng, W., Geng, L., Zhang, L., Liu, R., Chen, W., Yao, G., Zhang, H., Feng, X., Gao, X.*, et al.* (2015). Mesenchymal stem cells from patients with rheumatoid arthritis display impaired function in inhibiting Th17 cells. J Immunol Res *2015*, 284215.

Talwadekar, M.D., Kale, V.P., and Limaye, L.S. (2015). Placenta-derived mesenchymal stem cells possess better immunoregulatory properties compared to their cord-derived counterparts-a paired sample study. Sci Rep *5*, 15784.

Tamashiro, K.L., and Moran, T.H. (2010). Perinatal environment and its influences on metabolic programming of offspring. Physiol Behav *100*, 560-566.

Trounson, A., and McDonald, C. (2015). Stem Cell Therapies in Clinical Trials: Progress and Challenges. Cell Stem Cell *17*, 11-22.

Tsagias, N., Koliakos, I., Lappa, M., Karagiannis, V., and Koliakos, G.G. (2011). Placenta perfusion has hematopoietic and mesenchymal progenitor stem cell potential. Transfusion *51*, 976-985.

Uebel, K., Pusch, K., Gedrich, K., Schneider, K.T., Hauner, H., and Bader, B.L. (2014). Effect of maternal obesity with and without gestational diabetes on offspring subcutaneous and preperitoneal adipose tissue development from birth up to year-1. BMC Pregnancy Childbirth *14*, 138.

Wang, W., Deng, D., Li, J., and Liu, W. (2013). Elongated cell morphology and uniaxial mechanical stretch contribute to physical attributes of niche environment for MSC tenogenic differentiation. Cell Biol Int *37*, 755-760.

West, N.A., Kechris, K., and Dabelea, D. (2013). Exposure to Maternal Diabetes in Utero and DNA Methylation Patterns in the Offspring. Immunometabolism *1*, 1-9.

Yang, Y., Relan, N.K., Przywara, D.A., and Schuger, L. (1999). Embryonic mesenchymal cells share the potential for smooth muscle differentiation: myogenesis is controlled by the cell's shape. Development *126*, 3027-3033.

Zhu, Y., and Zhang, C. (2016). Prevalence of Gestational Diabetes and Risk of Progression to Type 2 Diabetes: a Global Perspective. Curr Diab Rep *16*, 7.

Table 1. Maternal and fetal characteristics.

	Healthy (*n*=9)	GDM (*n*=9)	*p* value
Age (years)	30.1 ± 1.68	30.1 ± 2.32	0.38
BMI (kg/m^2)	25.2 ± 1.76	32.4 ± 2.95	0.17
Gestational age (weeks)	38.7 ± 0.22	38 .0 ± 0.41	0.11
Infant weight (g)	3425 ± 85.43	3611 ± 151.5	0.09
Gender (female/male)	9/0	4/6[a]	
[a] Included one non-identical twins placenta			

Table 2. Primer sequences for genes of interest.

Gene	Forward Primer (5'-3')	Reverse Primer (5'-3')
ADIPOQ	AGGCCGTGATGGCAGAGATG	CTTCTCCAGGTTCTCCTTTCCTGC
CCL-17	CGGGACTACCTGGGACCTC	CCTCACTGTGGCTCTTCTTCG
CXCL-8	CTGGCCGTGGCTCTCTTG	CCTTGGCAAAACTGCACCTT
FOXC1	CACCCTCAAAGCCGAACTAA	GTTCGCTGGTGTGGTGAATA
GAPDH	ACTTCAACAGCACACCCACT	GCCAAATTCGTTGTCATACCAG
IL-1β	ATTCTCTTCAGCCAATCTTCA	TATCCCATGTGTCGAAGAAG
IL-10	TCAGCAGAGTGAAGACTTTC	CCTTGCTCTTGTTTTCACAG
IL-12	AAAGGACATCTGCGAGGAAAGTTC	CGAGGTGAGGTGCGTTTATGC
MRC1	ACCTCACAAGTATCCACACCATC	CTTTCATCACCACACAATCCTC
NANOG	CCCAGCCTTTACTCTTCCTACCAC	GATTCCTCTCCACAGTTATAGAAGGGA
OCT4	GTCCGAGTGTGGTTCTGTA	CTCAGTTTGAATGCATGGGA

PPARG	GCAGGAGATCTACAAGGACTTG	CCCTCAGAATAGTGCAACTGG
SOX7	CTGCTGAACTGGTCCCTAAC	TTGCGGGAAGTTGCTCTAA
SOX17	CCGCGGTATATTACTGCAACT	ACCCAGGAGTCTGAGGATTT
TBX6	CACTCCATGCACAAGTACCA	GCTGTCACGGAGATGAATGT
TNF	GATCCCTGACATCTGGAATCTG	GAAACATCTGGAGAGAGGAAGG

Figure legends

Figure 1. The morphology of human **(A)** H-/G-CMSCs and **(B)** AMSCs from primary culture to passage 2. Images of passage 0 were taken after seeding for 7 days; images of passage 1 and 2 were taken 5 days after subculture. **(C-D)** Analysis of cell morphology. Cell length of H-/G- CMSCs and AMSCs were measured from passage 0-2. **(E)** Cell surface area was measured at passage 2 of each group. Data was based on 150 cells per population, analysed by Image J, and results represent the mean ± SEM. Scale bar = 200 μm.

Figure 2. Lineage marker examination. The changes of pluripotent (*NANOG, OCT4*), endodermal (*SOX7, SOX17*), and mesodermal (*FOXC1, TBX6*) lineages markers in H-/G-CMSCs/AMSCs with increasing passage numbers were examined via real-time PCR. The data shown represent the mean ± SEM of 3 independent experiments.

Figure 3. Proliferation ability and immunophenotyping of Healthy- and GDM-CMSCs/AMSCs at passage 3. **(A)** Cell numbers were counted every two days for a 12-day period, indicating greater proliferative ability for CMSCs than AMSCs. Results are presented as mean from three replicates, n=6. $***p < 0.0001$, indicates statistical significance H-CMSCs vs. G-CMSCs; $###p < 0.0001$ indicates statistical significance H-AMSCs vs. G-AMSCs **(B)** Cell doubling time for CMSCs/AMSCs from healthy and GDM placenta was calculated based on cell counts at passage 3. Triplicates of each group were investigated in every placenta sample, n=9. **(C)** Metabolic activity (cell viability/proliferation) was assessed by measuring the MTT dye absorbance in a 12-day period. Cells from every donor were used to perform MTT assay and all assays were conducted in triplicate. OD was read at wavelength of 570 nm. Results represent mean ± SEM, n=6. **(D)** Immunophenotypic characterisation of H-/G- CMSCs and AMSCs. The graph compared the positive percentage of MSCs marker expressions in H-/G- CMSCs/AMSCs. Similar levels of CD marker expressions were observed in GDM and healthy MSC except for the marginally higher CD45

expression. The data represent the mean ± SEM of 5 independent experiments.

Figure 4. Differentiation potential of H-/G- CMSCs and AMSCs. **(A)** Representative images of tri-lineage differentiation of CMSCs and AMSCs derived from healthy and GDM placentas. Healthy- and GDM- CMSCs/AMSCs were induced to differentiate toward osteogenic lineage and stained with Alizarin red to identify calcified matrix, adipogenic lineage was verified by Oil-Red-O to identify lipid accumulation, and chondrogenic lineage was detected by Alcian blue staining. **(B)** Further analysis of adipogenic potential in H-/G-CMSCs/AMSCs was examined by Oil-Red-O stain after 21 day of differentiation. Scale bar = 200 μm. **(C)** Quantification of lipid accumulation by detecting the absorbance of Oil-Red-O extracts with isopropyl alcohol. The mean OD values represented the triplicates from 5 separate experiments. **(D)** Basal expression levels of *ADIPOQ* and **(E)** *PPARγ* were examined before inducing differentiation, n=8. Time course of adipogenic marker expressions – **(F)** *ADIPOQ* and **(G)** *PPARγ*, during differentiation process were analysed by qPCR. The data shown represent the mean ± SEM of 5 independent experiments.

Figure 5. Immunomodulatory effects of CMSCs and AMSCs derived from GDM and healthy placentas. Jurkat cells were cultured in the presence of healthy and GDM CMSCs/AMSCs CM **(A)** without activating with PMA/PHA or **(B)** with 50 ng/ml PMA and 5 μg/ml PHA. Cell proliferative ability was measured by MTT assay in a 5-day period. A significant reduction in Jurkat cell proliferation was observed, which showed more pronounced effect on suppressing cell proliferation by H-/G- CMSCs CM than H-/G- AMSCs CM. $^{\#}p < 0.001$ H-/G-CMSCs versus 10%FBS, $^{\wedge}p < 0.001$ H-/G-AMSCs versus 10%FBS **(C)** IL-2 secretion after PHA/PMA stimulation was measured by ELISA from day 0-3, which showed significantly diminished secretion of IL-2 in the presence of CMSCs/AMSCs CM. Results represent mean ± SEM of 5 independent experiments.

Figure 6. Healthy- and GDM- CMSCs/AMSCs modulate macrophage polarization through a

co-culture system. **(A)** A schematic diagram of the macrophage polarization procedure. THP-1 cells were pre-treated with PMA and either stimulated with IFN-γ/IL-4 or co-cultured with CMSCs/AMSCs. After co-culture for 24 h, cells were washed and RAN was extracted for gene expression analysis using qPCR for **(B-E)** M1 macrophage markers - *IL-1β, IL-12, CXCL8, TNF* and **(F-H)** M2 macrophage marker - *IL-10, MRC1, CCL-17* expressions. The data are expressed as fold changes of 6 independent experiments. Statistical significant indicates the relative expression compared to PMA-treated control(M0).

Figure 7. Cytokines secretion from PMA-THP1 in H-/G- CMSCs or AMSCs co-culture was examined by ELISA. **(A-B)** Supernatant was collected after 24 h and measured for secreted TNF-α and IL-10 expression levels. Results represent mean ± SEM of 6 independent experiments.

Supplementary Figure 1. Lineage markers examination in DMEM and DMEM/F12 culture. The changes of pluripotent (*NANOG, OCT4*), endodermal (*SOX7, SOX17*), and mesodermal (*FOXC1, TBX6*) lineages markers in H-/G-CMSCs/AMSCs with increasing passage numbers in two different growth media were examined via real-time PCR. The data shown represent the mean ± SEM of 3 independent experiments.

Supplementary Figure 2. Cell viability determined by trypan blue staining during a 12-day period. The percentage of cell death was calculated by counting blue-coloured cells (dead cell) from a total number of 100 cells in a haemocytometer. Results represent mean ± SEM of 6 independent experiments.

Supplementary Figure 3. Immunophenotypic characterisation of H-/G- CMSCs and AMSCs. The Table indicates the positive percentage of MSCs marker expressions in H-/G-

CMSCs/AMSCs at passage 2 and 3. The data represent the mean ± SEM of 5 independent experiments.

Supplementary Figure 4. Adipogenic potential in H-/G- CMSCs/AMSCs at early passages (passage1 and 2) was examined by Oil-Red-O stain after 21 day of differentiation. Cells were cultured in DMEM and induced adipogenesis by differentiation media. Scale bar = 100 μm. Quantification of lipid accumulation by detecting the absorbance of Oil-Red-O extracts with isopropyl alcohol. The mean OD values represented the triplicates from 3 independent experiments.

Highlights

- Chorionic MSCs have a longer morphological aspect and reduced surface area vs. amniotic MSCs.
- Chorionic MSCs display superior proliferation and tri-lineage differentiation potential vs. amniotic MSCs.
- GDM CMSCs display an enhanced adipogenic capacity in comparison to Healthy CMSCs.
- GDM MSCs and Healthy MSCs' secretome demonstrate the ability to supress IL-2 secretion and induce M2 macrophage polarisation.

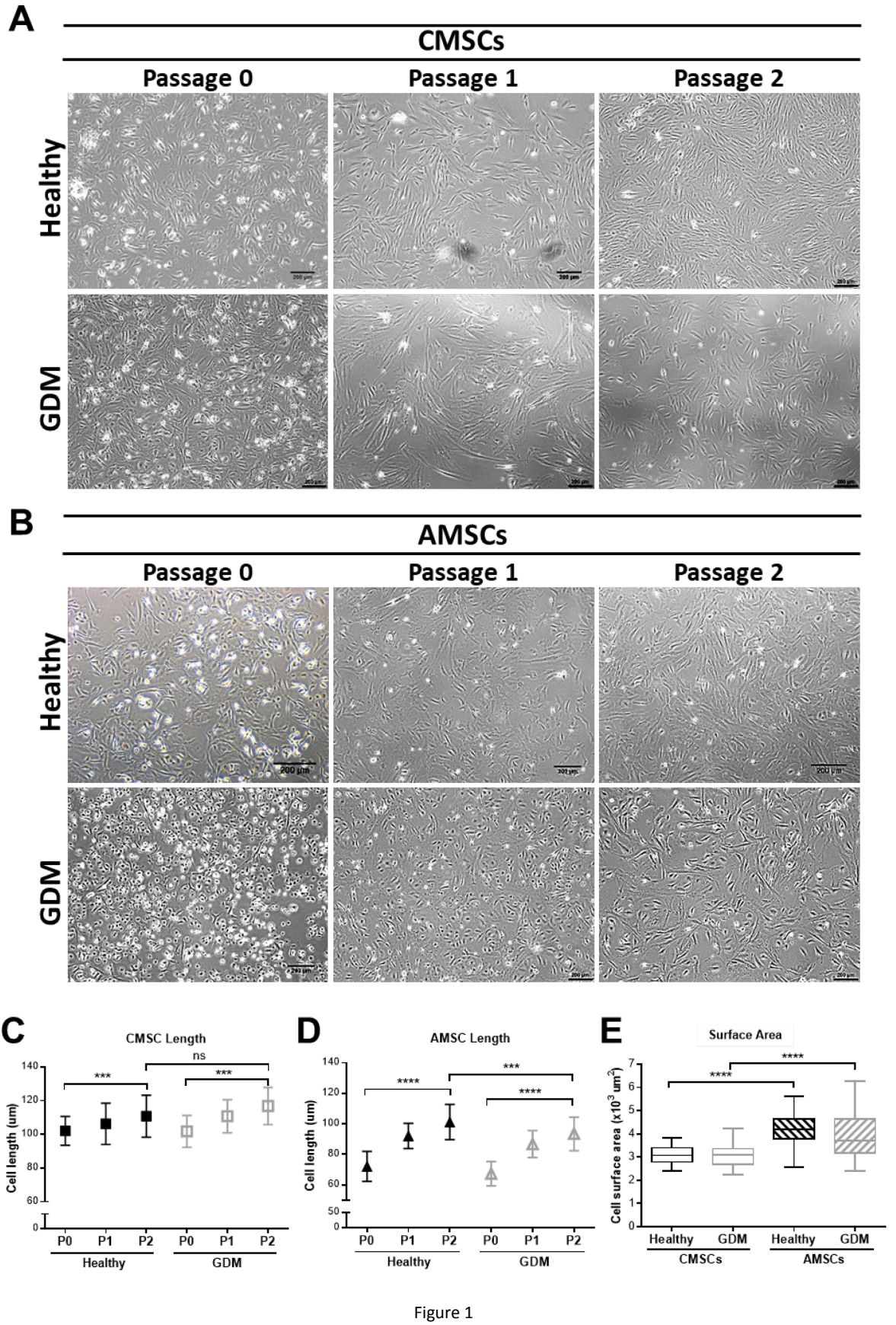
A
CMSCs
Passage 0
Passage 1
Passage 2
Healthy
GDM
B
AMSCs
Passage 0
Passage 1
Passage 2
Healthy
GDM
C
CMSC Length
ns
***
***
Cell length (um)
P0
P1
P2
P0
P1
P2
Healthy
GDM
D
AMSC Length
***
****
****
Cell length (um)
P0
P1
P2
P0
P1
P2
Healthy
GDM
E
Surface Area
****
****
Cell surface area (x10^3 um^2)
Healthy
GDM
Healthy
GDM
CMSCs
AMSCs

Figure 1

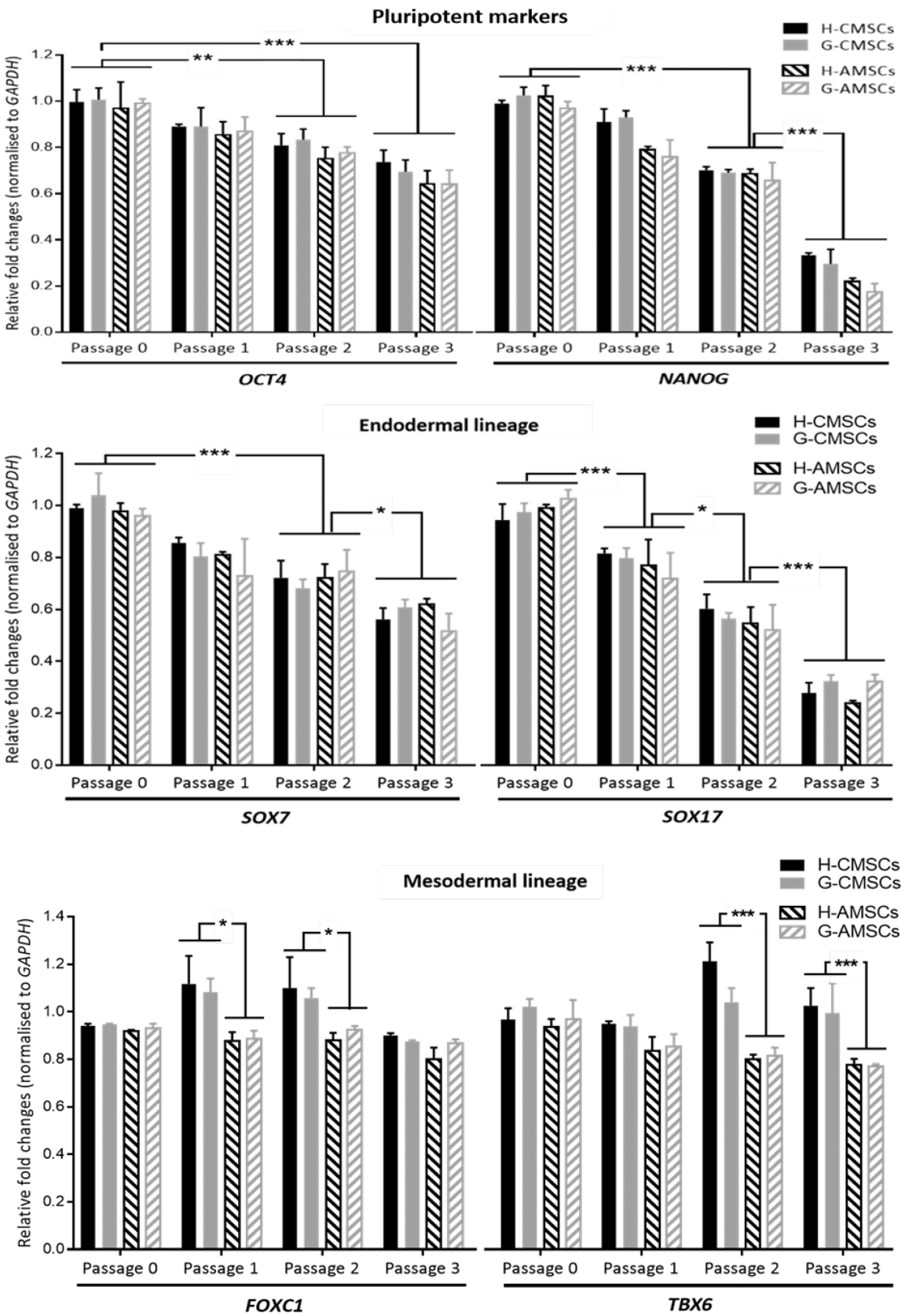
Pluripotent markers
H-CMSCs
G-CMSCs
H-AMSCs
G-AMSCs
Relative fold changes (normalised to GAPDH)
1.2
1.0
0.8
0.6
0.4
0.2
0.0
**
***
***
***
Passage 0
Passage 1
Passage 2
Passage 3
OCT4
NANOG
Endodermal lineage
H-CMSCs
G-CMSCs
H-AMSCs
G-AMSCs
Relative fold changes (normalised to GAPDH)
1.2
1.0
0.8
0.6
0.4
0.2
0.0
***
*
***
*
***
Passage 0
Passage 1
Passage 2
Passage 3
SOX7
SOX17
Mesodermal lineage
H-CMSCs
G-CMSCs
H-AMSCs
G-AMSCs
Relative fold changes (normalised to GAPDH)
1.4
1.2
1.0
0.8
0.6
0.4
0.2
0.0
*
*
***
***
Passage 0
Passage 1
Passage 2
Passage 3
FOXC1
TBX6

Figure 2

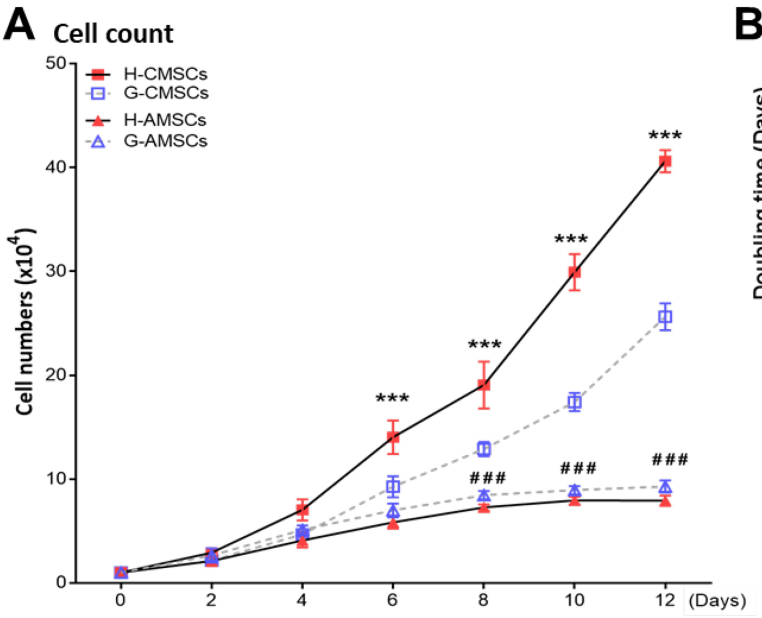

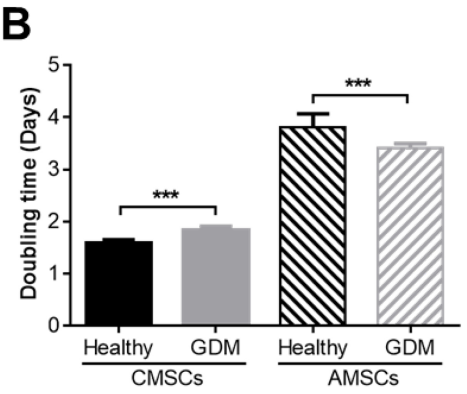

Average Doubling time (hours)

	CMSCs	AMSCs
Healthy	37.9	91.4
GDM	44.1	81.5

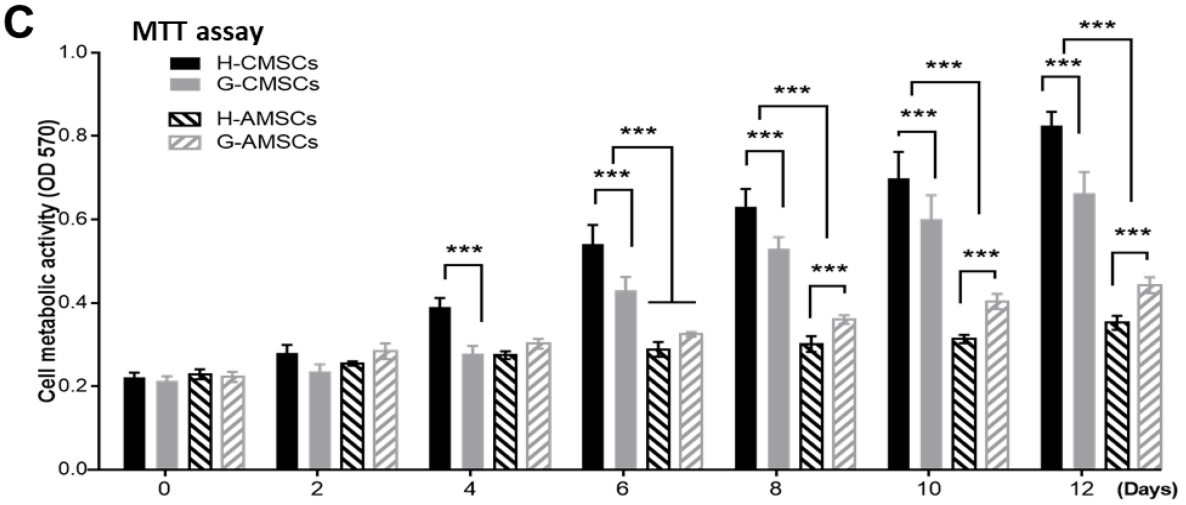

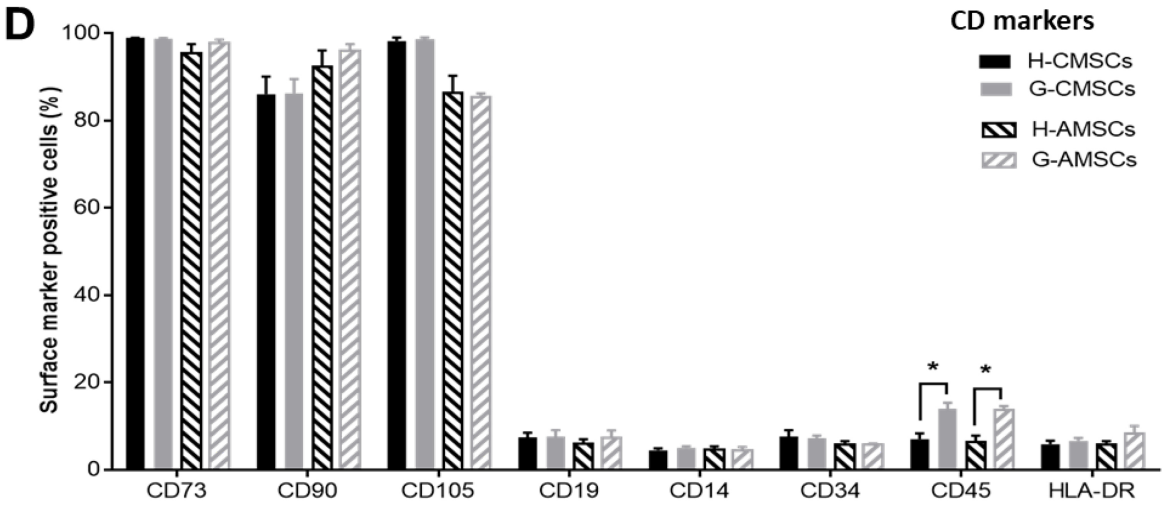

Figure 3

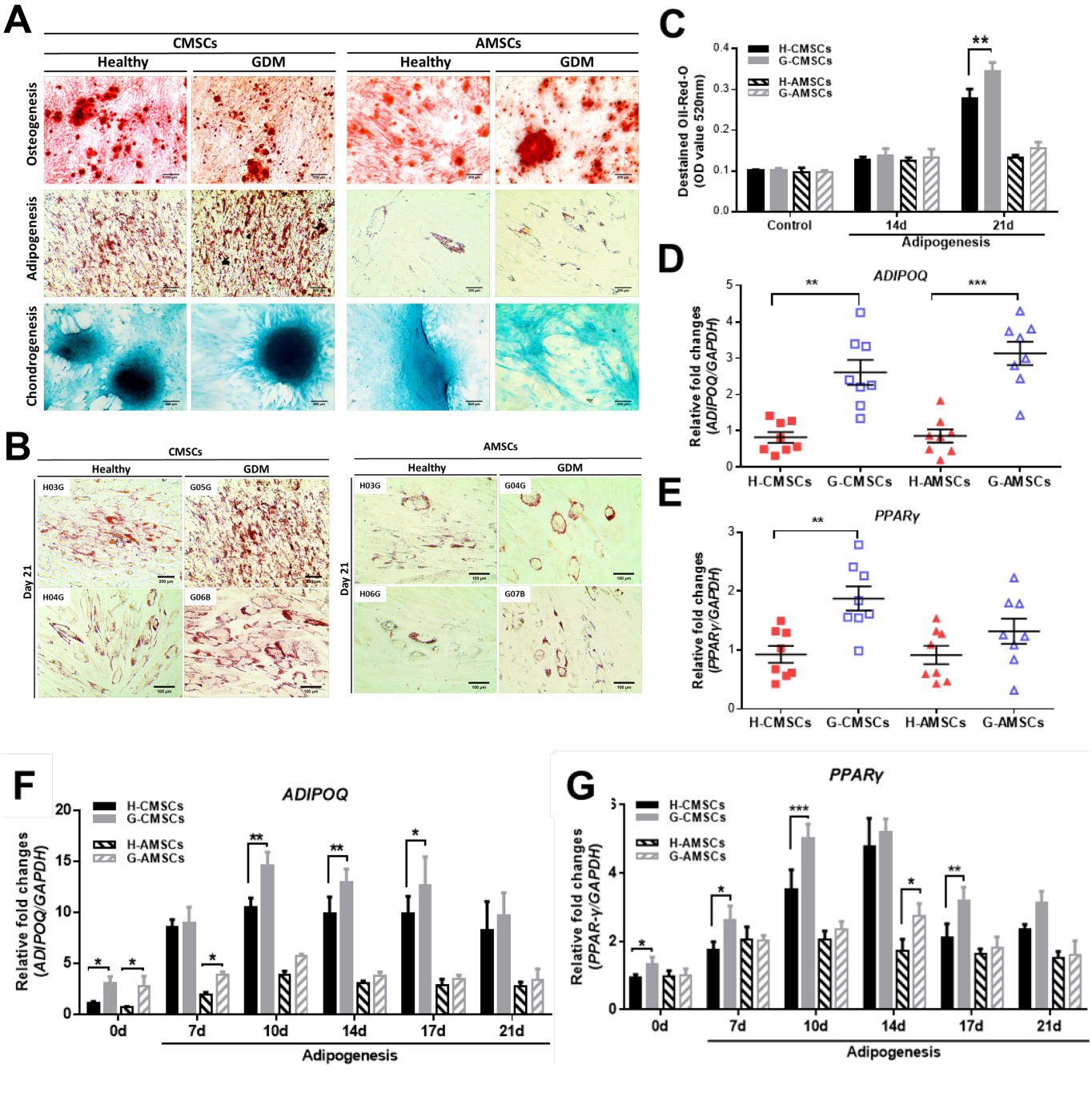
A
CMSCs
AMSCs
Healthy
GDM
Healthy
GDM
Osteogenesis
Adipogenesis
Chondrogenesis
B
CMSCs
AMSCs
Healthy
GDM
Healthy
GDM
Day 21
H03G
G05G
H04G
G06B
Day 21
H03G
G04G
H06G
G07B
C
H-CMSCs
G-CMSCs
H-AMSCs
G-AMSCs
Destained Oil-Red-O (OD value 520nm)
0.4
0.3
0.2
0.1
0.0
**
Control
14d
21d
Adipogenesis
D
ADIPOQ
Relative fold changes (ADIPOQ/GAPDH)
**
***
5
4
3
2
1
0
H-CMSCs
G-CMSCs
H-AMSCs
G-AMSCs
E
PPARγ
Relative fold changes (PPARγ/GAPDH)
**
3
2
1
0
H-CMSCs
G-CMSCs
H-AMSCs
G-AMSCs
F
ADIPOQ
H-CMSCs
G-CMSCs
H-AMSCs
G-AMSCs
Relative fold changes (ADIPOQ/GAPDH)
20
15
10
5
0
*
*
*
**
**
*
0d
7d
10d
14d
17d
21d
Adipogenesis
G
PPARγ
H-CMSCs
G-CMSCs
H-AMSCs
G-AMSCs
Relative fold changes (PPAR-γ/GAPDH)
6
4
2
0
*
*
***
*
**
0d
7d
10d
14d
17d
21d
Adipogenesis

Figure 4

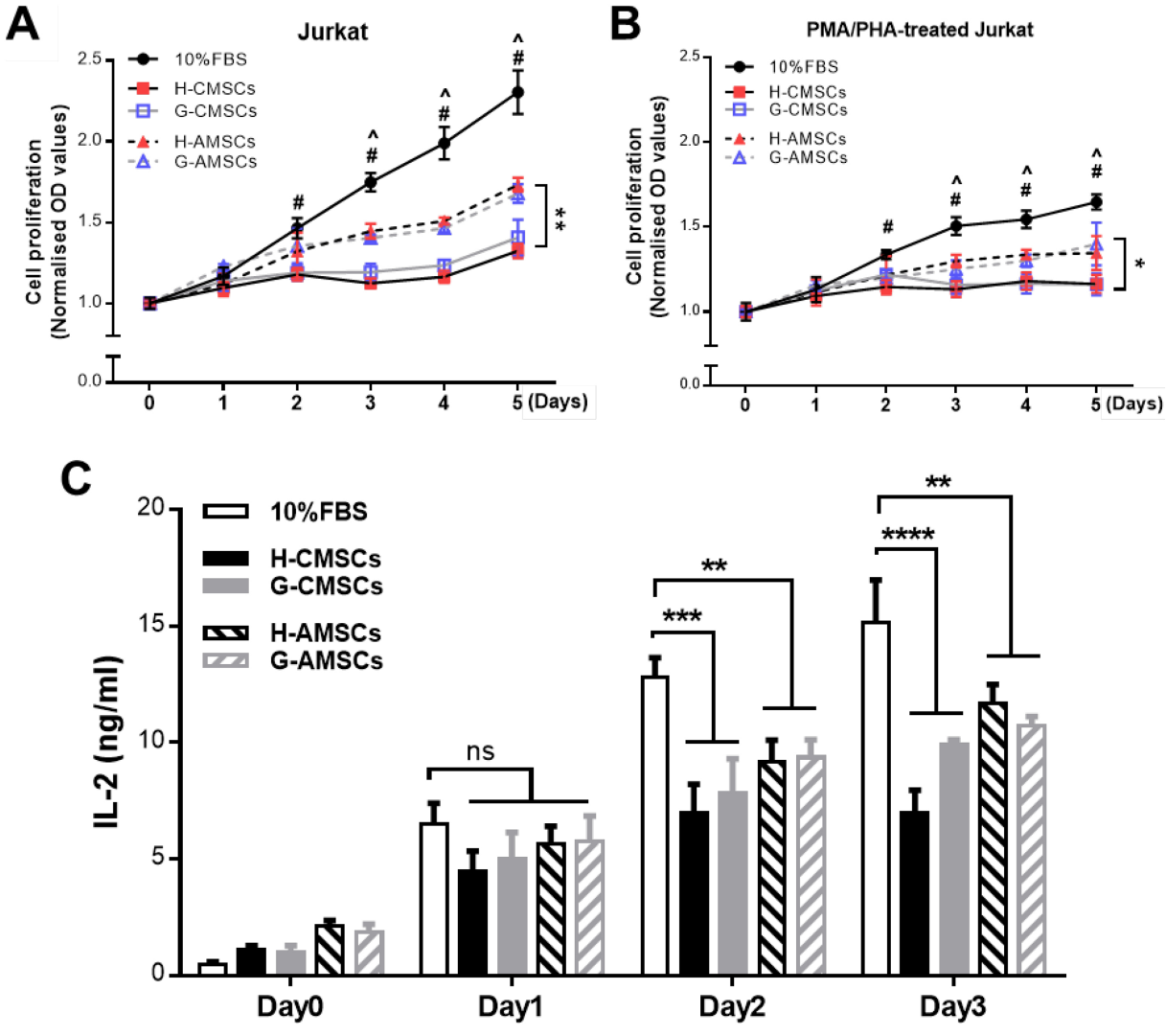
A
Jurkat
10%FBS
H-CMSCs
G-CMSCs
H-AMSCs
G-AMSCs
Cell proliferation
(Normalised OD values)
2.5
2.0
1.5
1.0
0.0
0
1
2
3
4
5 (Days)
#
^
#
^
#
^
#
**
B
PMA/PHA-treated Jurkat
10%FBS
H-CMSCs
G-CMSCs
H-AMSCs
G-AMSCs
Cell proliferation
(Normalised OD values)
2.5
2.0
1.5
1.0
0.0
0
1
2
3
4
5 (Days)
#
^
#
^
#
^
#
*
C
10%FBS
H-CMSCs
G-CMSCs
H-AMSCs
G-AMSCs
IL-2 (ng/ml)
20
15
10
5
0
ns
***
**
****
**
Day0
Day1
Day2
Day3

Figure 5

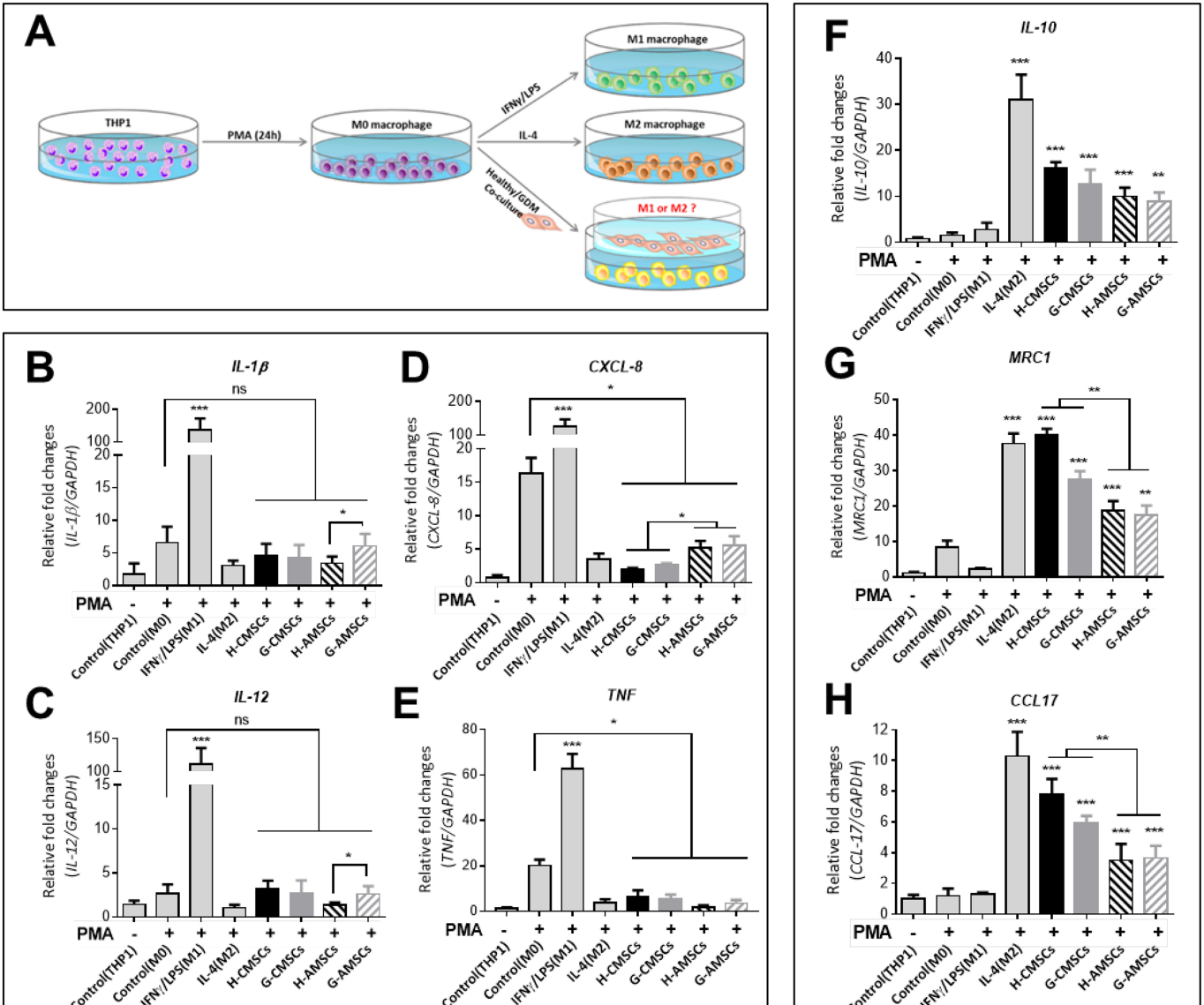
A
THP1
PMA (24h)
M0 macrophage
IFNγ/LPS
IL-4
Healthy/GDM Co-culture
M1 macrophage
M2 macrophage
M1 or M2 ?
B
IL-1β
ns
Relative fold changes (IL-1β/GAPDH)
C
IL-12
Relative fold changes (IL-12/GAPDH)
D
CXCL-8
Relative fold changes (CXCL-8/GAPDH)
E
TNF
Relative fold changes (TNF/GAPDH)
F
IL-10
Relative fold changes (IL-10/GAPDH)
G
MRC1
Relative fold changes (MRC1/GAPDH)
H
CCL17
Relative fold changes (CCL-17/GAPDH)
PMA
Control(THP1)
Control(M0)
IFNγ/LPS(M1)
IL-4(M2)
H-CMSCs
G-CMSCs
H-AMSCs
G-AMSCs

Figure 6

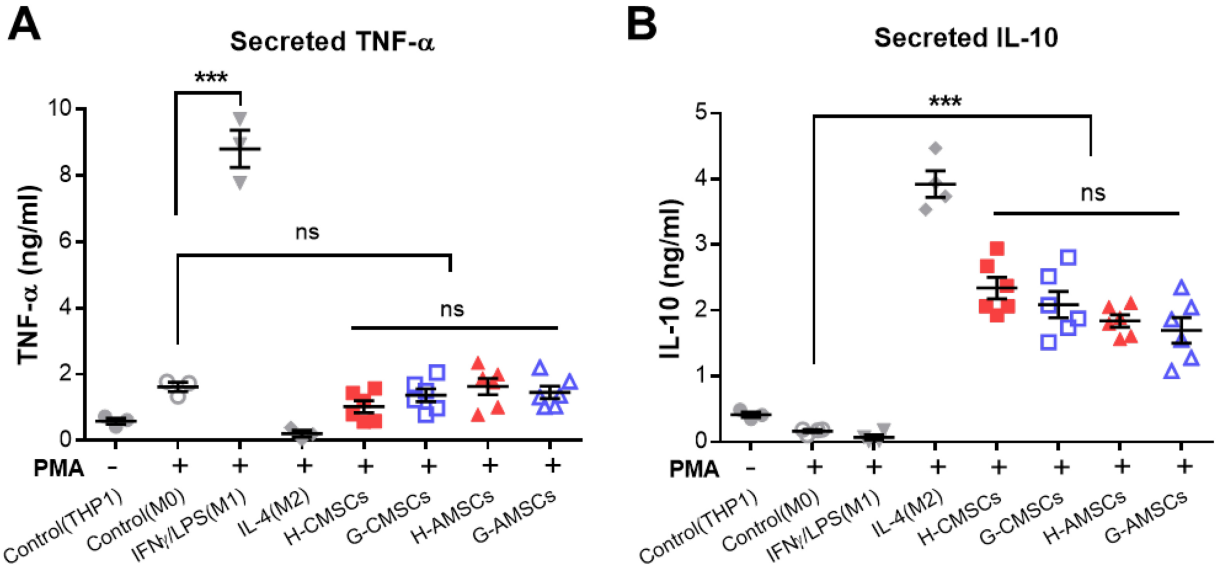
A
Secreted TNF-α
TNF-α (ng/ml)
10
8
6
4
2
0
***
ns
ns
PMA - + + + + + + +
Control(THP1)
Control(M0)
IFNγ/LPS(M1)
IL-4(M2)
H-CMSCs
G-CMSCs
H-AMSCs
G-AMSCs
B
Secreted IL-10
IL-10 (ng/ml)
5
4
3
2
1
0
***
ns
PMA - + + + + + + +
Control(THP1)
Control(M0)
IFNγ/LPS(M1)
IL-4(M2)
H-CMSCs
G-CMSCs
H-AMSCs
G-AMSCs

Figure 7